THE JOURNAL OF BIOLOGICAL CHEMISTRY
Vol. 278, No. 46, Issue of November 14, pp. 46007–46013, 2003
Printed in U.S.A.

Structural Basis of a Flavivirus Recognized by Its Neutralizing Antibody

SOLUTION STRUCTURE OF THE DOMAIN III OF THE JAPANESE ENCEPHALITIS VIRUS ENVELOPE PROTEIN*

Received for publication, July 18, 2003, and in revised form, August 29, 2003
Published, JBC Papers in Press, September 2, 2003, DOI 10.1074/jbc.M307776200

Kuen-Phon Wu‡§, Chih-Wei Wu‡§, Ya-Ping Tsao‡§, Ting-Wei Kuo‡, Yuan-Chao Lou‡, Cheng-Wen Lin‡, Suh-Chin Wu‡, and Jya-Wei Cheng‡¶

From the ‡Institute of Biotechnology and Department of Life Science, National Tsing Hua University, Hsinchu, Taiwan 300, Republic of China

The flavivirus envelope protein is the dominant antigen in eliciting neutralizing antibodies and plays an important role in inducing immunologic responses in the infected host. We have determined the solution structure of the major antigenic domain (domain III) of the Japanese encephalitis virus (JEV) envelope protein. The JEV domain III forms a β-barrel type structure composed of six antiparallel β-strands resembling the immunoglobulin constant domain. We have also identified epitopes of the JEV domain III to its neutralizing antibody by chemical shift perturbation measurements. Site-directed mutagenesis experiments are performed to confirm the NMR results. Our study provides a structural basis for understanding the mechanism of immunologic protection and for rational design of vaccines effective against flaviviruses.

Flaviviruses are small (50 nm) positive-strand RNA viruses that contain a lipid-bilayer membrane. Forty species of the flavivirus family have been associated with human diseases, and most of them are transmitted to their vertebrate hosts by infected mosquitoes or ticks (1). Among these, yellow fever, Japanese encephalitis, tick-borne encephalitis, and dengue are the most important viral arboviruses in the world. Japanese encephalitis virus is transmitted by mosquitoes and is widely distributed in Asia, including Japan, China, Taiwan, Korea, Philippines, the far eastern former Soviet Union, all of Southeast Asia, and India (1). There are about 50,000 cases and 10,000 deaths reported annually throughout Asia, but these numbers are believed to be greatly underestimated.

Like other flaviviruses, JEV[1] contains a single-stranded RNA genome of ~11 kb in size. The virion of JEV contains three structural proteins, a 12-kDa nucleocapsid or core protein, a 8-kDa non-glycosylated membrane protein, and a 53-kDa glycosylated envelope protein (E), as well as seven nonstructural proteins (NS1, NS2A, NS2B, NS3, NS4A, NS4B, NS5) (2). The E protein is the dominant antigen in eliciting neutralizing antibodies and plays an important role in inducing immunologic responses in the infected host (3). Structural elements of the E protein are also involved in viral attachment, fusion, penetration, hemagglutination, host range and cell tropism, and virus virulence and attenuation (1).

The three-dimensional structure of the TBEV E protein has been determined by x-ray crystallography (4). The x-ray structure reveals that the E protein forms a head-to-tail dimer with 170 Å in length. Each monomer of the E protein is composed of three discernible domains. Domain III containing the C-terminal 100 amino acids forms an Ig-like β-barrel structure composed of seven antiparallel β-strands. This domain is connected by a flexible region to domain I in the center, which folds into an eight-stranded antiparallel β-barrel. Domain I contains about 120 residues in three segments (residues 1–51, 137–189, and 285–302). The two long loops between these three segments form the dimerization domain II.

Recently, the structure of the E protein dimer of TBEV has been used to fit into the outer layer of density in the cryoelectron microscopy reconstruction of dengue virus (5). The structure suggests that the fusion mechanism of flaviviruses involves the insertion of the distal β-barrels of domain II of the E protein into the cellular membrane. On the other hand, the mechanism of antibody-mediated neutralization of the flavivirus remains a matter of speculation. Mutations on domain III of the E protein leading to the escape from antibody neutralization have been reported for JEV (6–9), louping ill virus (10), TBEV (11, 12), yellow fever virus (13), and dengue virus (14–16). Synthetic peptides have also been used to map the linear epitopes of domain III (17). However, none of these studies provide a detailed spatial configuration of the epitopes of domain III. To date, no structure has been reported for the E protein complexed with neutralizing antibodies. In this study, we have determined the solution structure of the domain III of the JEV E protein. In addition, we have identified the neutralizing epitopes of the JEV domain III to its monoclonal antibody (mAb E3.3) by comparing NMR chemical shifts of the free (14 kDa) and the antibody-bound (178 kDa) forms. Our results provide a structural basis for understanding the mechanism of immunologic protection and for rational design of vaccines effective against flaviviruses.

* This work is supported by grants from the National Science Council, ROC (NSC92-2113-M-007-026 and NSC91-3112-B-007-009) and the Program for Promoting Academic Excellence of Universities from the Ministry of Education, ROC (89-B-FA04-1-4). The costs of publication of this article were defrayed in part by the payment of page charges. This article must therefore be hereby marked "*advertisement*" in accordance with 18 U.S.C. Section 1734 solely to indicate this fact.

The atomic coordinates and structure factors (code 1PJW) have been deposited in the Protein Data Bank, Research Collaboratory for Structural Bioinformatics, Rutgers University, New Brunswick, NJ (http://www.rcsb.org/).

§ These authors contributed equally to this work.

¶ To whom correspondence should be addressed. Tel.: 886-3-5742763; Fax: 886-3-5738243; E-mail: jwcheng@life.nthu.edu.tw.

[1] The abbreviations used are: JEV, Japanese encephalitis virus; TBEV, tick-borne encephalitis virus; E protein, 53-kDa glycosylated envelope protein; mAb, monoclonal antibody; HSQC, heteronuclear single quantum coherence; TOCSY, total correlation spectroscopy; NOE, nuclear Overhauser effect; NOESY, nuclear overhauser enhancement spectroscopy; TROSY, transverse relaxation-optimized spectroscopy.

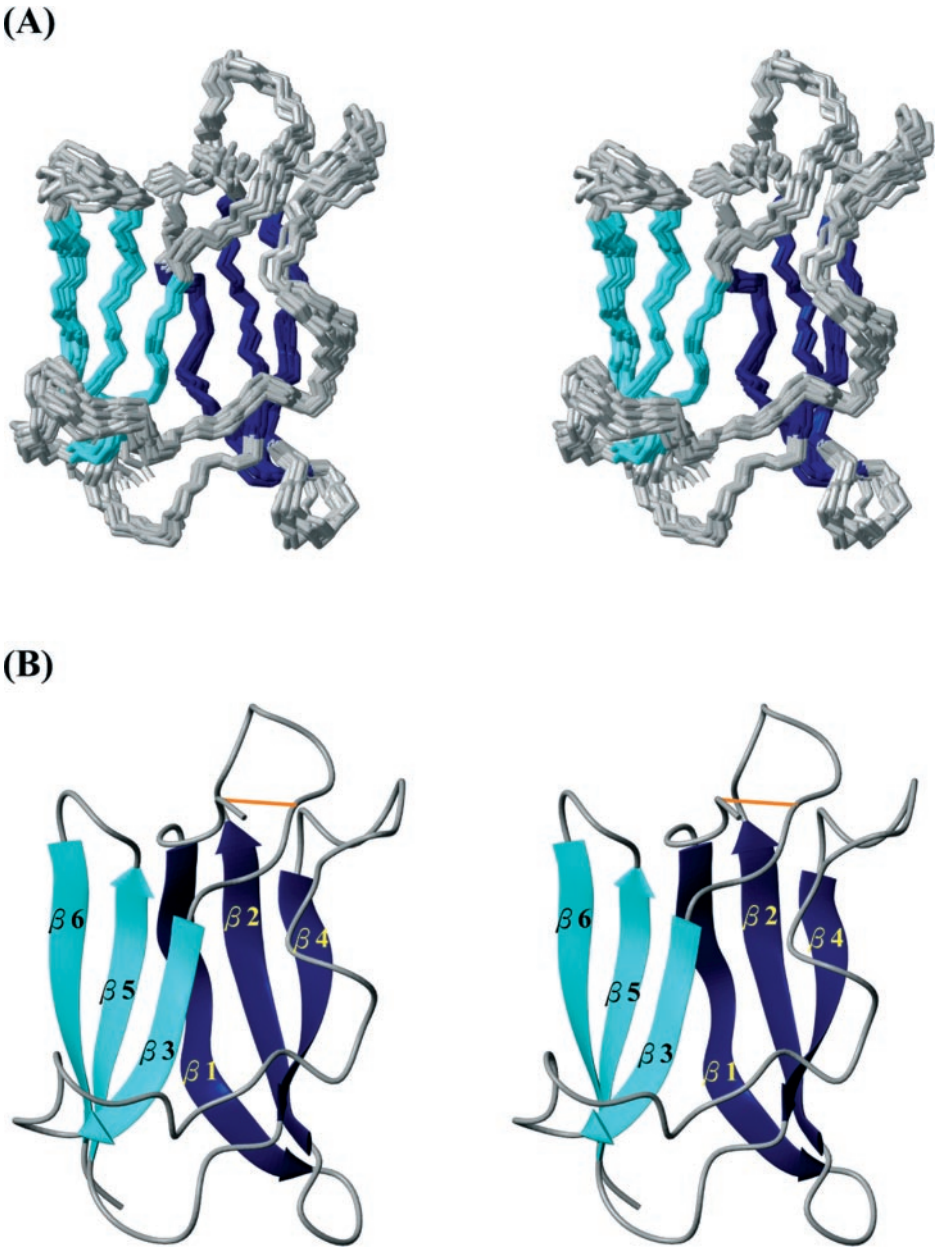

FIG. 1. **Solution structure of the JEV domain III.** *A*, a stereo view of the backbone superimposition of the final 15 structures. *B*, ribbon diagram of the lowest energy structure of the JEV domain III. The *orange stick* represents the disulfide bridge between residues 304 and 335.

EXPERIMENTAL PROCEDURES

Protein Preparation and Purification—The DNA fragments encoding residues 292–402 of the domain III of the JEV (CH2195LA) E protein were amplified by PCR. The amplified PCR products were subcloned into pET-22b vector. Plasmids encoding JEV domain III were introduced into *Escherichia coli* strains BL21(DE3), and transformants were cultured overnight at 37 °C in SOB medium supplemented with ampicillin (100 μg/ml). The uniform ^{15}N-labeled and/or ^{15}N/^{13}C-labeled samples were expressed in cells grown in M9 minimal media containing $^{15}NH_4Cl$ and/or (U-^{13}C) glucose. For preparation of the (U-^{2}H, ^{15}N)-domain III for NMR spectroscopy, the protein was expressed in the M9 minimal media with 99% D_2O in place of H_2O and $^{15}NH_4Cl$ as a sole nitrogen source (18). The cell lysates were centrifuged, and the supernatant from the centrifugation was applied to a nickel-nitrilotriacetic acid column according to the protocols provided by the manufacturer (Qiagen Inc.) at 4 °C. Fractions containing the JEV domain III were pooled, concentrated, and added to a 1.6 × 60.0 cm Sephacryl S-100 column (Amersham Biosciences). Finally, the protein was eluted with NMR buffer containing 50 mM K_2HPO_4 (pH 6.5), 100 mM NaCl, 10 mM NaN_3, and 0.1 mM EDTA. Purity of the protein was confirmed by high pressure liquid chromatography and mass spectroscopy. The final protein concentration for NMR study was 2 mM in 90% H_2O, 10% D_2O. To prepare D_2O samples, concentrated protein solutions were lyophilized and redissolved in D_2O.

Monoclonal Antibody Preparation—The hybridoma cell line producing mAb E3.3 was prepared from BALB/c mice immunized with JEV Beijing-1 strain. The specificity of mAb E3.3 was demonstrated previously on JEV E protein (8, 19), showing >95% plaque neutralization against Beijing-1 strain and blocking viral hemagglutination at the reciprocal titer of 320.

NMR Spectroscopy—All NMR data used in the structural analysis were acquired with Bruker Avance 600 or 500 MHz spectrometers equipped with triple resonance probes at 25 °C. TROSY spectra were performed on a Bruker Avance 800 MHz spectrometer with a sample (JEV domain III/mAb E3.3) concentration of 100 μM at 25 °C. ^{1}H NMR data were referenced to the ^{1}H resonance frequency of 2,2-dimethyl-2-silapentanesulfonic acid; ^{13}C and ^{15}N resonances were referenced indirectly by multiplying the proton frequency by 0.25144953 for ^{13}C and 0.101329118 for ^{15}N (20, 21). The NMR experiments performed included two-dimensional ^{1}H-^{15}N HSQC, ^{1}H-^{13}C HSQC, three-dimensional ^{15}N-NOESY-HSQC, HNCO, HN(CA)CO, HN(CO)CA, HNCA, CBCA(CO)NH, and HNCACB for backbone assignments, ^{15}N-TOCSY-HSQC, HCC(CO)NH-TOCSY, HCCH-TOCSY, HCCH-COSY, HBHA-(CO)NH for side chain assignments (22). All spectra were processed with the program XWIN-NMR 2.6 and NMRPipe and analyzed using NMRView 5.04. $^{3}J_{HNH}$ coupling constants were estimated from the HNHA experiment. H/D exchange rates of the amide protons were

TABLE I
Summary of structural constrains and structure statistics

NOE restraints	763
Intraresidues (i − j = 0)	205
Sequential (i − j = 1)	263
Medium range (2 ≤ i − j ≤ 4)	43
Long range (i − j > 4)	206
Hydrogen bond constraints	46
Dihedral angles[a]	194
Structural Statistics (15 Structures)	
NOE violations, number > 0.3 Å	0
Dihedral angel violations, number > 5°	0
r.m.s.d.[b] for geometrical analysis	
Bond lengths (Å)	0.0018 ± 0.00003
Bond angles (degree)	0.502 ± 0.0035
Impropers (degree)	0.378 ± 0.0026
r.m.s.d. from experimental restraints	
Distance (Å)	0.0214 ± 0.00065
Dihedral angles (deg.)	0.472 ± 0.082
Atomic r.m.s.d. for protein[c]	
All heavy atoms	1.428
Backbone	0.682
Atomic r.m.s.d. for structured region[d]	
All heavy atoms	1.278
Backbone	0.464
Ramachandran statistics	
Most favored region (%)	72.0
Additionally allowed (%)	26.5
Generously allowed (%)	1.4
Disallowed (%)	0.1

[a] Dihedral angles were predicted from the program TALOS.
[b] r.m.s.d., root mean square deviation.
[c] Only residues 12–107 were shown.
[d] Residues in the structured region are as follows: 308–316, 322–328, 339–343, 369–374, 381–386, 391–396.

determined by recording a series of HSQC spectra in several time intervals after the proteins had been dissolved in D_2O.

Experimental Restraints—NOE-based distance restraints were collected from analysis of three-dimensional ^{15}N-edited NOESY-HSQC and ^{13}C-edited NOESY-HSQC spectra recorded with mixing times of 150 and 80 ms, respectively. NOEs were broadly categorized as "strong," "medium," and "weak," corresponding to distance limits of 1.8–2.8, 1.8–3.4, and 1.8–5.0 Å, respectively. NOE restraints involving methyl group and pseudoatoms were corrected by relaxing 0.3 Å to take into account equivalent atoms.

The ϕ and ψ angles were obtained based on $^3J_{HNH\alpha}$ coupling constants derived from the HNHA experiment and predicted from TALOS (23). Hydrogen bond restraints were included in calculations only if the amide protons were slowly exchanging and if the β-strand inter-strand NOE cross-peaks were observed. Each hydrogen bond was enforced by two distance restraints of 1.8–2.3 Å (amide proton to carbonyl oxygen) and 2.8–3.3 Å (amide nitrogen to carbonyl oxygen).

Structure Calculation—The structure calculations were carried out using the X-PLOR 3.851 (24) program on a SuSE Linux 7.3 PC equipped with an Intel Pentium 4 1.8 GHz CPU and 512 MB DDR-SDRAM. The structures were calculated and refined with *ab initio* simulated annealing protocol, "sa.inp," and SA refinement protocol, "refine.inp" in X-PLOR 3.851. All force constants and molecular parameters, etc. were set to their default values, as in the original sa.inp and refine.inp protocols, with the exception of the timestep (ps), which was decreased to 0.001 ps throughout the calculations. Simulated annealing was performed using 9,000 steps at 1,000 K and 10,000 steps by gradually cooling to 100 K. Finally, these structures were energy-minimized using 500 steps of Powell energy minimization. The best 15 lowest energy structures were further analyzed with MOLMOL (25) and PROCHECK-NMR (26). These final structures contained no distance constraint violations greater than 0.3 Å and no dihedral angle constraint violations greater than 5°. The coordinates of both the representative structure and the family of structures have been deposited at the Brookhaven Protein Data Bank (access number 1PJW).

RESULTS AND DISCUSSION

Structure Determination—The JEV domain III is well behaved at millimolar concentrations and well suited for solution structural studies using modern NMR techniques. The backbone ^{1}H, ^{15}N, ^{13}C, and ^{13}CO assignments of the 111 residue JEV domain III are essentially complete. More than 85% of the side chain ^{1}H resonances are assigned. A total of 763 NOE-derived distance constraints, including 205 intraresidue, 263 sequential, 43 medium (1 < i − j < 5), 206 long range (i − j ≥ 5), and 46 hydrogen bond distance restraints in conjunction with 194 backbone dihedral angles are used in the structure calculations. The overlay of the backbone atoms for the 15 lowest energy structures of the JEV domain III is shown in Fig. 1*A*. Fig. 1*B* shows the ribbon diagram of the lowest energy structure of the JEV domain III. The energetic and structural statistics are listed in Table I. The root mean square deviation calculated from the averaged coordinates for the JEV domain III is 0.68 Å for the backbone heavy atoms (N, C, and Cα) and 1.43 Å for all heavy atoms. Analysis of ϕ and ψ backbone angles is facilitated by using the program Procheck_NMR (26). Only 0.1% of the residues are in disallowed regions, and more than 98% of the residues are within most favored or additional allowed regions of the Ramachandran plot.

Structure Description and Homology—The JEV domain III forms a β-barrel type structure composed of six antiparallel β-strands resembling the immunoglobulin constant domain (Fig. 1*B*). The six β-strands consist of residues 308–316, 322–328, 339–344, 369–374, 381–386, and 391–396. A conserved disulfide bridge is found between residues Cys-304 and Cys-335. The top of the β-barrel is closed by the N-terminal residues and the loops between the β2-β3, β3-β4, and β5-β6 strands. The amino acid sequence of the JEV domain III is 37.1% identical and 65.0% similar to that of the TBEV domain III, and the global fold of the JEV domain III is similar to that of the TBEV domain III (4). In the JEV domain III, strands β1, β2, β3, β4, β5, and β6 correspond to strands A, B, C, E, F, and G of the TBEV domain III (4). However, there are localized differences between these two proteins. Formation of extra strands (Ax, Cx, Dx, and D in Fig. 2*b* of Rey *et al.* (4)) has been observed in the TBEV domain III. These extra strands, except strand D, are all located in the loop regions on the top of the β-barrel. Strand D is found in the long loop region between strands β3 and β4. Since the x-ray structure of the TBEV E protein has been determined to be a head-to-tail dimer, contacts between domain III and domains I and II from the other subunit may force the loop regions to form more ordered conformations. We have used reduced spectral density functions to analyze the NMR relaxation rates and ^{1}H-^{15}N heteronuclear NOEs of the JEV domain III (data not shown) (27, 28). Our results indicate that the loop regions, especially the β3-β4 loop, undergo picosecond fast motions, as evident from the larger J(H) values. Thus, the ordered conformations are less favored in these loop regions of the JEV domain III. However, more ordered conformations could not be ruled out in the full-length JEV E protein.

Epitope Mapping by NMR—Antibody-antigen interactions play important roles in the immune system. Identification of an epitope is the first step toward the elucidation of the molecular mechanism underlying antibody-antigen interactions. Series of short peptides encompassing the sequences of a protein antigen can be used to locate the antibody binding sites. However, exhaustive mutagenesis experiments are needed to identify the epitope if an epitope is comprised of discontinuous fragments. Alternatively, NMR can be used to map an epitope (29, 30). Chemical shifts are highly sensitive to the local magnetic environment and are excellent probes for conformational change. Previously, the chemical shift perturbation method has been shown to accurately identify the epitopes of several antibody-bound antigens (29, 31, 32). JEV domain III gives a well resolved ^{1}H-^{15}N HSQC spectrum in which backbone amide peaks for most of the residues can be identified (Fig. 2*A*). However, low sample concentrations due to the limited availability of mAb E3.3 and the size of the JEV domain III/mAb E3.3 com-

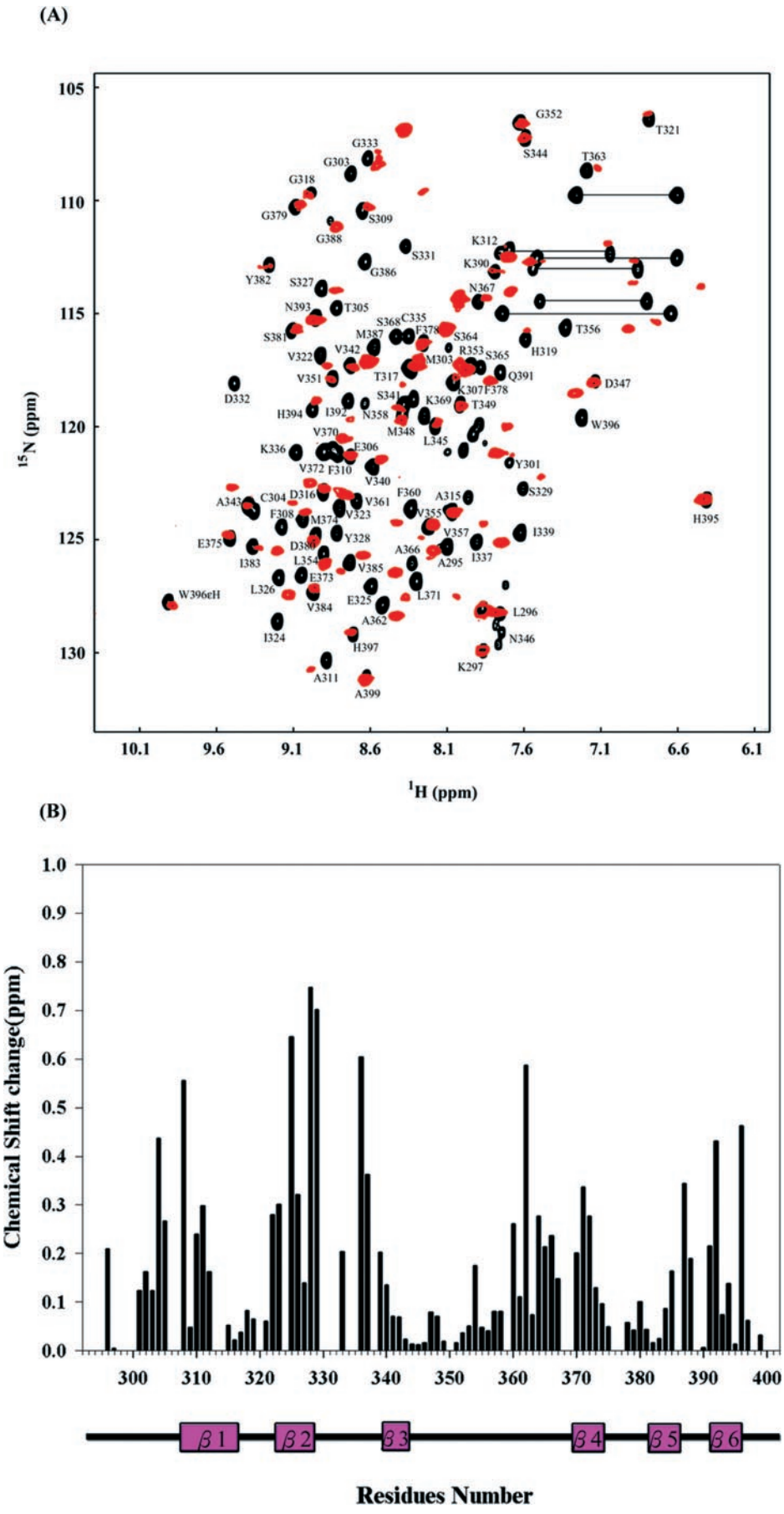

FIG. 2. *A*, overlay of the ^{1}H-^{15}N HSQC spectrum of the JEV domain III (*black*) and the ^{1}H-^{15}N TROSY spectrum of the JEV domain III/mAb E3.3 complex (*red*). Cross-peaks are labeled according to the residue types and numbers. *B*, chemical shift change *versus* residue number of the JEV domain III upon mAb E3.3 binding. The chemical shift changes are calculated according to the equation: $\Delta\delta = [0.5 \times [\Delta\delta(^{1}H)^{2}] + [0.2 \times [\Delta\delta(^{15}N)^{2}]]]^{1/2}$.

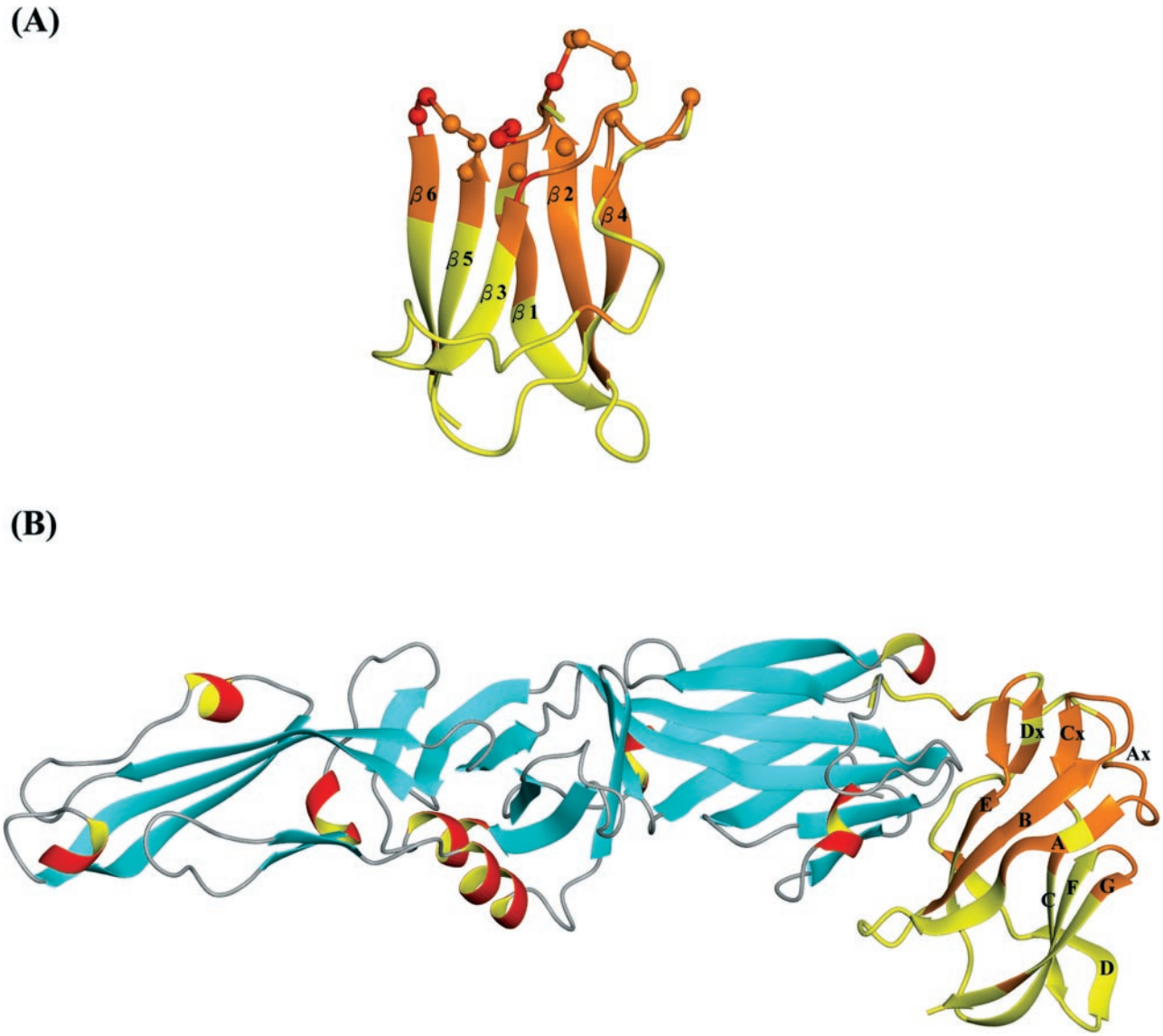

FIG. 3. *A*, the location of residues whose ^{1}H-^{15}N cross peak positions are affected by the formation of the JEV domain III/mAb E3.3 complex. The color scheme used is: *orange*, a residue whose peak shows chemical shift change $\Delta\delta \geq 0.15$ ppm; *red*, a residue whose peak exhibits a significantly reduced intensity at the same position as in the free spectrum and has been reported to be the mutation site. Mutations leading to the escape from antibody neutralization or neutralizing epitopes mapped by phage-displayed peptide libraries are represented as *dots*. *B*, chemical shift changes of the JEV domain III/mAb E3.3 complex mapped onto the three-dimensional structure of the TBEV E protein (Protein Data Bank access number 1SVB). The TBEV domain III is shown in *yellow*, and the residues analogous to the JEV domain III, which have significant chemical shift changes upon antibody binding, are shown in *orange*. Structural elements (strands A, B, C, D, E, F, G, Ax, Cx, Dx) are labeled according to Fig. 2 of Rey *et al.* (4).

plex (178 kDa) still hinder the NMR studies. Fortunately, with the deuteration of the protein sample (33) and the recently developed TROSY-based NMR techniques (34, 35), most of the ^{1}H-^{15}N cross-peaks seen in the free JEV domain III remain resolved in the TROSY spectrum of the JEV domain III/mAb E3.3 complex (Fig. 2*A*). Comparison of the ^{1}H-^{15}N cross-peaks in the free and the antibody-bound forms show that complex formation causes significant chemical shift changes for a discrete set of resonances including residues 302–312, 322–339, 360–372, and 385–392 (Fig. 2*B*). The residues with significant chemical shift changes upon binding with mAb E3.3 are mapped onto the structure of the JEV domain III, as shown in Fig. 3*A*. Basically, the mapped epitopes are located on the top portion of the β-barrel including residues in the N termini, the β2-β3, β3-β4, and the β5-β6 loops. Residues close to the top portion of the β-barrel on the six β-strands are also found to have large chemical shift changes upon mAb E3.3 binding. The mapped epitopes of the JEV domain III are presented in the three-dimensional structure of the TBEV E protein to demonstrate the relative positions of the antibody binding sites of the domain III to domains I and II of the E protein (Fig. 3*B*). It has been suggested that the CFG strands of the TBEV domain III, which form the outer lateral surface of the dimer (Fig. 3*B*), may be the antigenic sites (4). However, our studies of the JEV domain III show that the top portion of the β-barrel, including residues in the N termini, the β2-β3, β3-β4, β5-β6 loops, and the adjacent residues on the six β-strands, are the major neutralizing antibody binding sites. Previously, mutations that lead to the escape from antibody neutralization have been reported for the JEV domain III (Fig. 4*A*) (6–9,17). These mutation sites are all located in the N termini, the β2-β3, β3-β4, and the β5-β6 loops on the top of the β-barrel covered by the NMR mapped epitopes.

Site-directed Mutagenesis—To further confirm the NMR mapped epitopes, we have performed site-directed mutagenesis experiments on residues 337, 352, 360, and 387. Residues 337

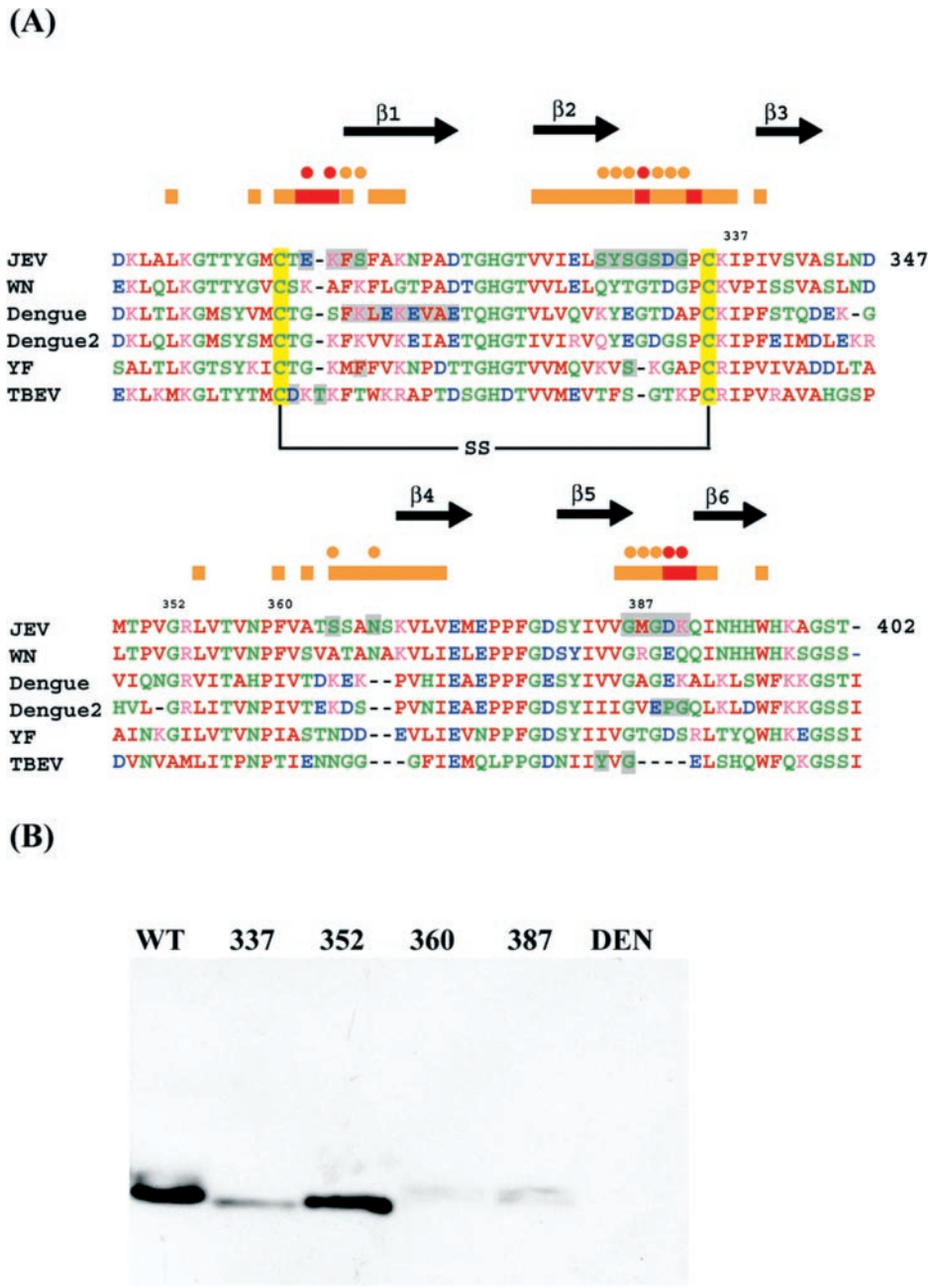

FIG. 4. *A*, a structure-based multiple sequence alignment of the domain III of JEV, West Nile (*WN*), Dengue, Dengue2, yellow fever (*YF*), and TBEV. Secondary structural elements are shown *above* the alignment. Mutations leading to the escape from antibody neutralization or neutralizing epitopes mapped by phage-displayed peptide libraries found in the JEV domain III are represented by *dots*. *Rectangular bars* denote regions mapped by chemical shift changes of the JEV domain III/mAb E3.3 complex. The color schemes of Fig. 3 are used. *Shaded residues* represent the mutations escaped from antibody neutralization or neutralizing epitopes mapped by phage-displayed peptide libraries for the domain III of JEV, West Nile, Dengue, Dengue2, yellow fever, and TBEV. Residues 337, 352, 360, and 387 studied by site-directed mutagenesis are shown *above* the sequence alignment. *B*, Western blot analysis of mAb E3.3 binding to the wild-type, I337A, G352A, F360A, and E387A proteins. The Dengue virus domain III is used as a control.

and 360 are located in the β2-β3 and β3-β4 loops close to the top of the β-barrel but have not been reported to be involved in the neutralizing antibody binding. Residue 387, which has been suggested to be the antigenic site (17), is located in the β5-β6 loop. These three residues are chosen because they all exhibit significant chemical shift changes upon mAb E3.3 binding, and they are located in the three major antigenic loops (Fig. 2*A*). Although residue 352 is located in the β3-β4 loop, it does not show any chemical shift change upon mAb E3.3 binding. Thus, mutation of residue 352 is expected to have little influence on the antibody binding. Based on the Western blot analysis, the I337A, F360A, and R387A mutations all exhibit significant reductions of binding to the neutralizing antibody mAb E3.3 (Fig. 4*B*). On the other hand, the G352A mutation shows little change on binding to mAb E3.3 as compared with the wild type protein. The site-directed mutagenesis results correlate well with the NMR mapped epitopes on the JEV domain III.

Biological Importance—The E protein of the flaviviruses is involved in viral attachment, fusion, penetration, hemagglutination, host range and cell tropism, and virus virulence and attenuation (1). Among the three structural domains, domain III is the major antigenic domain of the E protein. Single mutations in the domain III of a number of flaviviruses are responsible for changes in the above mentioned properties. Mutations leading to the escape from antibody neutralization or neutralizing epitopes mapped by phage-displayed peptide libraries have been reported on residues 306, 331, 333, and 386–390 of JEV (6–9), residues 308, 310, and 311 of louping ill virus (10), residues 384 and 386 of TBEV (11, 12), residue 305 of yellow fever virus (13), and residues 307, 333–351, and 383–389 of the dengue viruses (14–16). Fig. 4*A* shows mutation sites that abolish binding of the corresponding neutralizing antibodies of various flaviviruses. Not surprisingly, most of the mutation sites are covered by the NMR mapped epitopes of the JEV domain III (Fig. 4*A*). Because of the sequence homology and the similar global fold between the JEV and TBEV domain III, a common three-dimensional structure of the domain III for

all flaviviruses can be predicted. Moreover, because the mutation sites that abolish binding of the corresponding neutralizing antibodies of various flaviviruses are covered by the present NMR mapped epitopes, it can be anticipated that the neutralizing epitopes on the domain III of different flaviviruses are located within the similar regions. To further understand the mechanism of antibody-mediated neutralization of the flaviviruses, NMR structural studies and epitope mapping of the domain III of the dengue virus are currently under way in our laboratory.

In conclusion, NMR structural studies and site-directed mutagenesis were performed to identify and characterize the neutralizing epitopes of the JEV domain III. Our results provide a structural basis for understanding the mechanism of immunologic protection and for rational design of vaccines effective against flaviviruses.

Acknowledgments—We thank Dr. Yi-Ling Lin (Academia Sinica) for providing us the DNA strain of the dengue domain III and Dr. R. Weiseman (Bruker) for acquiring the TROSY spectra (800 MHz) for us. We also thank Drs. Shiou-Ru Tzeng and Ju-Pi Li for helpful discussions. This study was carried out on the 600 MHz NMR spectrometer at the Regional Instrument Center at Hsinchu, National Science Council, Taiwan.

REFERENCES

1. Burke, D. S., and Monath, T. P. (2001) *Fields Virology,* 4th Ed., pp. 1043–1125, Lippincott Williams & Wilkins, Philadelphia
2. Chambers, T. J., Hahn, C. S., Galler, R., and Rice, C. M. (1990) *Annu. Rev. Microbiol.* **44,** 649–688
3. McMinn, P. C. (1997) *J. Gen. Virol.* **78,** 2711–2722
4. Rey, F. A., Heinz, F. X., Mandl, C., Kunz, C., and Harrison, S. C. (1995) *Nature* **375,** 291–298
5. Kuhn, R. J., Zhang, W., Rossmann, M. G., Pletnev, S. V., Corver, J., Lenches, E., Jones, C. T., Mukhopadhyay, S., Chipman, P. R., Strauss, E. G., Baker, T. S., and Strauss, J. H. (2002) *Cell* **108,** 717–725
6. Cecilia, D., and Gould, E. A. (1991) *Virology* **181,** 70–77
7. Seif, S. A., Morita, K., Matsuo, S., Hasebe, M. F., and Igarashi, A. (1995) *Vaccine* **13,** 1515–1521
8. Wu, S. C., Lian, W. C., Hsu, L. C., and Liau, M. Y. (1997) *Virus Res.* **51,** 173–181
9. Lin, C. W., and Wu, S. C. (2003) *J. Virol.* **77,** 2600–2606
10. Jiang, W. R., Lowe, A., Higgs, S., Reid, H., and Gould, E. A. (1993) *J. Gen. Virol.* **74,** 931–935
11. Holzmann, H., Heinz, F. X., Mandl, C. W., Guirakhoo, F., and Kunz, C. (1990) *J. Virol.* **64,** 5156–5159
12. Holzmann, H., Stiasny, K., Ecker, M., Kunz, C., and Heinz, F. X. (1997) *J. Gen. Virol.* **78,** 31–37
13. Schlesinger, J. J., Chapman, S., Nestorowicz, A., Rice, C. M., Ginocchio, T. E., and Chambers, T. J. (1996) *J. Gen. Virol.* **77,** 1277–1285
14. Lin, B., Parrish, C. R., Murray, J. M., and Wright, P. J. (1994) *Virology* **202,** 885–890
15. Hiramatsu, K., Tadano, M., Men, R., and Lai, C. J. (1996) *Virology* **224,** 437–445
16. Roehring, J. T., Bolin, R. A., and Kelly, R. G. (1998) *Virology* **246,** 317–328
17. Wu, S. C., and Lin, C. W. (2001) *Virus Res.* **76,** 59–69
18. Leiting, B., Marsilio, F., and O'Connell, J. F. (1998) *Anal. Biochem.* **265,** 351–355
19. Wu, S. C., Lian, W. C., Hsu, L. C., Wu, Y. C., and Liau, M. Y. (1998) *Virus Res.* **55,** 83–91
20. Wishart, D. S., Bigam, C. G., Yao, J., Abildgaard, F., Dyson, H. J., Oldfield, E., Markley, J. L., and Sykes, B. D. (1995) *J. Biomol. NMR* **6,** 135–140
21. Markley, J. L., Bax, A., Arata, Y., Hilbers, C. W., Kaptein, R., Sykes, B. D., Wright, P. E., and Wuthrich, K. (1998) *J. Biomol. NMR* **12,** 1–23
22. Ferentz, A. E., and Wagner, G. (2000) *Q. Rev. Biophys.* **33,** 29–65
23. Cornilescu, G., Delaglio, F., and Bax, A. (1999) *J. Biomol. NMR* **13,** 289–302
24. Brunger, A. T. (1993) *X-PLOR Version 3.1: A system for X-Ray Crystallography and NMR*, Yale University Press, New Haven, CT
25. Koradi, R., Billeter, M., and Wuthrich, K. (1996) *J. Mol. Graph.* **14,** 51–55
26. Laskowski, R. A., Rullmannn, J. A., MacArthur, M. W., Kaptein, R., and Thornton, J. M. (1996) *J. Biomol. NMR* **8,** 477–486
27. Farrow, N. A., Zhang, O., Szabo, A., Torchia, D. A., and Kay, L. E. (1995) *J. Biomol. NMR* **6,** 153–162
28. Lefevre, J. F., Dayie, K. T., Peng, J. W., and Wagner, G. (1996) *Biochemistry* **35,** 2674–2686
29. Tashiro, M., and Montelione, G. T. (1995) *Curr. Opin. Struct. Biol.* **5,** 471–481
30. Saito, N. G., and Paterson, Y. (1996) *Methods* (*Orlando*) **9,** 516–524
31. Huang, X., Yang, X., Luft, B. J., and Koide, S. (1998) *J. Mol. Biol.* **281,** 61–67
32. Ding, W., Huang, X., Yang, X., Dunn, J. J., Luft, B. J., Koide, S., and Lawson, C. L. (2000) *J. Mol. Biol.* **302,** 1153–1164
33. Markus, M. A., Dayie, K. T., Matsudaira, P., and Wagner, G. (1994) *J. Magn. Reson. Ser. B* **105,** 192–195
34. Pervushin, K., Riek, R., Wider, G., and Wuthrich, K. (1997) *Proc. Natl. Acad. Sci. U. S. A.* **94,** 12366–12371
35. Fiaux, J., Bertelsen, E. B., Horwich, A. L., and Wuthrich, K. (2002) *Nature* **418,** 207–211